System-Level Analysis for Full-Duplex MmWave Cellular Networks

Christodoulos Skouroumounis, Constantinos Psomas, and Ioannis Krikidis
KIOS Research and Innovation Center of Excellence,
Department of Electrical and Computer Engineering, University of Cyprus, Cyprus
Email: {cskour03, psomas, krikidis}@ucy.ac.cy

***Abstract*—In this paper, we investigate the performance of full-duplex (FD) radio in large-scale heterogeneous millimeter-wave (mmWave) cellular networks. The FD radio can potentially double the spectral efficiency but its performance is compromised by the existence of loop- and multi-user interference compared to half-duplex radio. Using stochastic geometry tools, we derive closed-form expressions for the coverage probability and the sum-rate performance of the considered network. We evaluate the impact of the FD radio on the network performance and quantify the associated gains under different network parameter settings. Our results demonstrate that the combination of FD radio with heterogeneous mmWave cellular networks provides significant gains, since it increases the spectral efficiency but also alleviates the effects of the multi-user interference.**

***Index Terms*—Full-duplex, millimeter wave, heterogeneous networks, stochastic geometry.**

I. Introduction

The exponential growth of wireless data services along with the spectrum shortage motivate the investigation of the next-generation cellular networks. Aiming at increasing the network throughput, next-generation networks will have to combine several innovative techniques, such as full-duplex (FD) radio and millimeter wave (mmWave) communications [1].

FD radio refers to the simultaneous operation of both transmission and reception using non-orthogonal channels, which can potentially double the spectral efficiency with respect to the half-duplex (HD) counterpart [2]. Nevertheless, the non-orthogonal operation creates a loop interference (LI) between the output and the input antennas. Owing to the overwhelming effect of LI at a transceiver, FD has been previously regarded as an unrealistic approach. However, recent advances in transceiver design and signal processing tend to make LI cancellation feasible [2]. Another key challenge in implementing the FD radio in large-scale networks, is the mitigation of the severe multi-user interference caused by the FD operation. Several research efforts have been carried out to study the effect of loop- and multi-user interference on the FD performance for large-scale wireless networks, and several techniques have been proposed to alleviate the additional interference caused by the FD technology. The performance of FD small-cells in ultra-dense networks was studied in [3] and the beneficial effect of multiple antennas in mitigating the interference introduced by the FD operation demonstrated. Hybrid HD/FD cellular networks are studied in [4], where the authors considered both cell-center and cell-edge users; it is demonstrated that FD base stations (BSs) with HD users provide higher performance than FD BSs and FD users.

MmWave communication is also a key enabling technology for the next-generation wireless communications owing to its abundant spectrum resources, which would lead to multi-Gbps rates [10]. Recent studies have shown that the unique features of mmWave communications, such as directivity, sensitivity to blockages, and higher path losses, cause a positive effect on the network performance, which is the natural suppression of the overall interference. Thus, the co-design of FD radio and mmWave networks is of critical importance in order to combat the severe multi-user interference caused by the FD technology by exploiting the prominent properties of mmWave communications. Even though FD radio is well-investigated for below 6 GHz applications, there is minimal research on the effects of higher frequencies, i.e. mmWaves. In [6], the authors proposed a model to explore the viability of FD over the mmWave band. The implementation of FD-mmWave communication network in the context of ultra-dense small cell networks with relay nodes is investigated in [7].

In this paper, we study the achieved coverage and sum-rate performance of heterogeneous FD-mmWave cellular networks, where the users operate either in the FD or HD mode. The main contribution of this paper is the co-design of FD radio and mmWave heterogeneous cellular networks, which can be mutually beneficial, since FD can provide high network throughput and mmWaves can lead to multi-user interference mitigation. We propose an analytical framework based on stochatsic geometry that captures the impact of FD radio on the coverage and sum-rate performance of the considered system, for different network parameters. By deriving analytical expressions of the coverage and sum-rate performance, we show that mmWave cellular networks can indeed significantly improve the coverage and sum-rate performance of the FD systems. To the best of our knowledge, this is the first work which incorporates FD radio in a mmWave cellular network from a stochastic geometry point-of-view.

This work was supported by the Research Promotion Foundation, Cyprus, under the project INFRASTRUCTURES/1216/0017, and by the EU's Horizon 2020 programme under the Marie Skodowska-Curie grant agreement No 690750.

II. System model

We consider a heterogeneous mmWave cellular network composed by K network tiers of BSs. The locations of the BSs belonging to the k-th tier, where $k \in \{1, ..., K\}$, are modeled by a homogeneous Poisson Point Process (PPP) Φ_k with density λ_k. Each BS is assumed to serve a single scheduled user that is independently and uniformly distributed in its Voronoi cell. Specifically, we assume that the locations of the users form a homogeneous PPP Ψ with density λ_1, which is the baseline assumption for many cellular system studies [8]. We consider the scenario where both BSs and users can operate either in FD mode or in HD mode. A BS belonging to the k-th tier, operates in FD mode based on the predefined probability π_k^{F}, while a user is operating in FD mode with probability δ^{F}. An HD user can either operate in DL or in UL mode, with probabilities δ^{D} and δ^{U}, respectively.

We further assume the employment of multiple transmit/receive antennas at both the BSs and the users, and we approximate the actual beam pattern using a sectorized model [9]. Both the transmit and receive beam patterns are parameterized by three values: main lobe beamwidth $\theta \in [0, 2\pi]$, main lobe gain M, and side lobe gain m. Therefore, the gain of an interference link seen by a user, is a discrete random variable and is given by $G = \{M^2, Mm, m^2\}$ with the corresponding probabilities $p_G = \left\{\left(\frac{\theta}{\pi}\right)^2, 2\left(\frac{\theta}{\pi}\right)\left(\frac{\pi-\theta}{\pi}\right), \left(\frac{\pi-\theta}{\pi}\right)^2\right\}$. We assume the active link between each user and its associated BS lies in the boresight direction of the antennas of both terminals [9].

A. Channel and blockage model

The signals are assumed to experience both large-scale path-loss effects and small-scale fading. Specifically, the small-scale fading between two nodes is Rayleigh distributed. Thus, the power of the channel fading between a user and a BS located at X, is an exponential random variable with unit mean, i.e. $h_X \sim \exp(1)$. We also assume the independence of small-scale Rayleigh fading for each link. For the large-scale path-loss, we assume the unbounded singular path-loss model, $L(x, y) = \|x - y\|^{-a}$ which assumes that the received power decays with the distance between the transmitter x and the receiver y, where $a > 2$ denotes the path-loss exponent. Regarding the LI, we assume that the FD-capable users and BSs employ imperfect cancellation mechanisms [2]. As such, we consider the residual LI channel coefficient to follow a Nagakami-μ distribution with parameters $\left(\mu, \sigma_{\mathrm{LI}}^2\right)$, where $\frac{1}{\sigma_{\mathrm{LI}}^2}$ characterizes the LI cancellation capability of both the BSs and the users. Therefore, the power gain of the residual LI channel follows a Gamma distribution with mean μ and variance $\frac{\sigma_{\mathrm{LI}}^2}{\mu}$, i.e. $h_{\mathrm{LI}} \sim \Gamma\left(\mu, \frac{\sigma_{\mathrm{LI}}^2}{\mu}\right)$. Moreover, all wireless links exhibit additive white Gaussian noise with variance σ_n^2.

The link between a transmitter and a receiver can be either in line-of-sight (LOS) or in non-LOS (NLOS), each with a different path-loss exponent. We consider the *LOS ball* model proposed in [10], where the LOS and NLOS probability functions are modeled as a simple step function $\mathcal{P}_{\mathrm{L}} = \mathbb{1}_{r \le R}$ and $\mathcal{P}_{\mathrm{N}} = \mathbb{1}_{r > R}$, respectively, where $\mathbb{1}_X$ is the indicator function of X with $\mathbb{1}_X = 1$ if X is true, otherwise $\mathbb{1}_X = 0$, R is the maximum length of a LOS link [10]. The path-loss exponent $a(r)$ for the link between a BS located at distance r from a UE, is modeled as a discrete random variable and is equal to $a(r) = a_{\mathrm{L}}$ if $r \le R$, otherwise $a(r) = a_{\mathrm{N}}$.

B. Power allocation

We assume that all users utilize distance-proportional fractional power control in order to compensate the large-scale path-loss and maintain the average received signal power at their corresponding serving BSs equal to ρ. To accomplish this, a user, which is at a distance d from its serving BS, adapts its transmitted signal power to $\rho d^{a(d)\epsilon}$, where $0 \le \epsilon \le 1$ is the power control fraction. It is important to note here that if $\epsilon = 1$, the path loss is completely compensated, and if $\epsilon = 0$, no channel inversion is performed and all the users transmit with the same power. For the DL transmission, we consider a fixed power transmission scheme. All the BSs belonging in the k-th tier, transmit with power P_k, where $P_i > P_j$, if $i < j$.

III. FD-mmWave cellular network

A. Association criteria

We assume weighted path-loss user association criteria for both the DL and the UL transmission. In the case where the user operates in FD mode, it can be either served simultaneously by two different BSs for DL and UL transmission or served by a single FD BS for both DL and UL transmissions. Let χ_k denote the BS with minimum path-loss from the k-th tier. For a user at $y \in \mathbb{R}^2$, the association criteria for the DL and UL transmission, are given by

$$x_{\mathrm{D}} = \underset{x \in \{\chi_k\}}{\arg\min} \frac{D_k}{L(x, y)}, \text{ and } x_{\mathrm{U}} = \underset{x \in \{\chi_k\}}{\arg\min} \frac{U_k}{L(x, y)}. \quad (1)$$

where $\chi_k = \arg\min_{x \in \Phi_k} L(x, y)^{-1}$, D_k and U_k are the weight factors for the DL and UL transmission, respectively, and $k \in \{1, \ldots, K\}$. Each user associates with the BS that offers the strongest received power for the DL transmission and the closest BS for the UL transmission. Thus, the DL and UL weight factors are equal to $D_k = P_k^{-1}$ and $U_k = \rho$, respectively [9]. For the case where a user is served by a single BS for the DL and UL transmission, this BS must satisfy both expressions in (1) as well as operate in FD mode.

Let p_{ij}, where $i < j$, denote the joint association probability that a user is served by a BS from the i-th tier in the DL and a BS from the j-th tier in the UL. Furthermore, let p_i^{D} and p_i^{U} be the probabilities that an HD user is served by a BS from the i-th tier for DL and UL, respectively. The following lemmas characterize the aforementioned probabilities.

Lemma 1. *An FD user is served by a BS from the i-th tier in the DL and a BS from the j-th tier in the UL with probability*

$$p_{ii} = \lambda_i \left(\frac{1 - e^{-R^2 \pi \sum_{k=1}^{K} \lambda_k \mathcal{D}_{ik}(a_{\mathrm{L}})}}{\sum_{k=1}^{K} \lambda_k \mathcal{D}_{ik}(a_{\mathrm{L}})} + \frac{e^{-R^2 \pi \sum_{k=1}^{K} \lambda_k \mathcal{D}_{ik}(a_{\mathrm{N}})}}{\sum_{k=1}^{K} \lambda_k \mathcal{D}_{ik}(a_{\mathrm{N}})} \right),$$

when $i = j$, and with probability (3)*, when $i \neq j$, where $\mathcal{D}_{ik}(\alpha) = \max\{P_k/P_i, 1\}^{2/\alpha}$, $\eta_{ij}(u, v) = \left(u^{a(u)} P_j / P_i\right)^{a(v)}$, and $\mathcal{K}_{ik}(\alpha, \beta) = \pi \max\left\{u^{\alpha} P_k / P_i, v^{\beta}\right\}^{2/\alpha} \lambda_k$.*

$$p_{ij}=4\pi^2\lambda_i\lambda_j\left(\underbrace{\int_0^R\int_{\eta_{ij}(u,v)}^R uve^{-\sum\limits_{k=1}^{K}\mathcal{K}_{ik}(a_{\mathrm{L}},a_{\mathrm{L}})}dvdu}_{\text{LOS } x_{\mathrm{D}} \text{ and LOS } x_{\mathrm{U}}}+\int_R^\infty\left(\underbrace{\int_{\eta_{ij}(u,v)}^u ve^{-\sum_{k=1}^{K}\mathcal{K}_{ik}(a_{\mathrm{N}},a_{\mathrm{L}})}dv}_{\text{NLOS } x_{\mathrm{D}} \text{ and LOS } x_{\mathrm{U}}}+\underbrace{\int_{\eta_{ij}(u,v)}^u ve^{-\sum\limits_{k=1}^{K}\mathcal{K}_{ik}(a_{\mathrm{N}},a_{\mathrm{N}})}dv}_{\text{NLOS } x_{\mathrm{D}} \text{ and NLOS } x_{\mathrm{U}}}\right)u\,du\right). \quad (3)$$

Proof. The proof follows similar steps as in [9]. The main difference lies in the fact that here the area around a user is divided into two regions, the LOS and NLOS region, where different path-loss exponents are applied. Based on the association criteria given by (1), the serving BSs of a user for the DL and UL transmission can be either: (i) both in LOS, (ii) both in NLOS, (iii) or NLOS and LOS, respectively. A detailed proof is omitted due to space limitations. □

Lemma 2. *An HD user is served by a BS from the i-th tier for the DL and UL, with probability*

$$p_i^{\mathrm{D}}=\lambda_i\left(\frac{1-e^{-R^2\pi\sum_{k=1}^{K}\left(\frac{P_k}{P_i}\right)^{\frac{2}{a_{\mathrm{L}}}}\lambda_k}}{\sum_{k=1}^{K}\left(\frac{P_k}{P_i}\right)^{\frac{2}{a_{\mathrm{L}}}}\lambda_k\pi}+\frac{e^{-R^2\sum_{k=1}^{K}\left(\frac{P_k}{P_i}\right)^{\frac{2}{a_{\mathrm{N}}}}\lambda_k}}{\sum_{k=1}^{K}\left(\frac{P_k}{P_i}\right)^{\frac{2}{a_{\mathrm{N}}}}\lambda_k\pi}\right),$$

and $p_i^{\mathrm{U}}=\lambda_i\left(\sum_{k=1}^{K}\lambda_k\right)^{-1}$, *respectively.*

Proof. The proof follows similar steps as in Lemma 1, except that in this case we are studying the DL and UL transmissions separately. From Lemma (1), we can obtain the DL's probability expression, by setting $\mathcal{D}_{ik}(\alpha)=(P_k/P_i)^{\frac{2}{\alpha}}$ and the UL's probability expression by setting $\mathcal{D}_{ik}(\alpha)=1$. □

We also need to derive the joint probability density function (PDF) of the distance to the serving BSs for DL and UL transmissions for the users operating in FD mode. The following lemma provides the joint distance distribution.

Lemma 3. *The joint PDF of the distance between an FD user and its serving BS(s) that belong in the i-th and the j-th tier for the DL and the UL transmission, is given by*

$$f(r_i,r_j)=\begin{cases}2\pi\lambda_i r_i e^{-\sum_{k=1}^{K}\pi\lambda_k\mathcal{D}_{ik}(a(r_i))r_i^2}, & i=j,\\ 4\pi^2\lambda_i\lambda_j r_i r_j e^{-\sum_{k=1}^{K}\mathcal{K}_{ik}(a(r_i),a(r_j))}, & i\neq j.\end{cases}$$

Proof. Similarly as the procedure of Lemma 1, the joint cumulative distribution function (CDF) can be obtained by considering two more conditions, i.e. $x_{\mathrm{D}}>r_i$ and $x_{\mathrm{U}}>r_j$. Then the joint PDF can be obtained by differentiation. □

B. SINR Distribution

In this section, we characterize the overall signal-to-interference-plus-noise ratio (SINR) complimentary CDF. Without loss of generality and by following Slivnyak's theorem, we execute the analysis for a typical user located at the origin. The SINR can be expressed as follows

$$\mathrm{SINR}_{ij}^{D}=\frac{M^2P_ix_{\mathrm{D}}^{-a(x_{\mathrm{D}})}|h_{x_{\mathrm{D}}}|^2}{I^{\mathrm{D}}+\mathbb{1}_{\mathrm{FD}}I_{\mathrm{LI}}^{\mathrm{D}}+\sigma_n^2}, \quad (4)$$

$$\mathrm{SINR}_{ij}^{U}=\frac{M^2P_u(x_{\mathrm{U}})x_{\mathrm{U}}^{-a(x_{\mathrm{U}})}|h_{x_{\mathrm{U}}}|^2}{I^{\mathrm{U}}+\mathbb{1}_{\mathrm{FD}}I_{\mathrm{LI}}^{\mathrm{U}}+\sigma_n^2}, \quad (5)$$

where $x_{\mathrm{D}}\in\Phi_i$ and $x_{\mathrm{U}}\in\Phi_j$ are the serving BSs for the DL and the UL transmissions, respectively, and $\mathbb{1}_{\mathrm{FD}}$ is the indicator function for the event "typical user is FD-capable". $I^{\mathcal{S}}$, where $\mathcal{S}\in\{\mathrm{D},\mathrm{U}\}$, represents the received interference in $\mathcal{S}$ transmission, and is given by

$$I^{\mathcal{S}}=\Pi^b\sum\nolimits_{u\in\Phi_k\setminus\{x_{\mathcal{S}}\}}\sum\nolimits_G GP_ku^{-a(u)}h_u + \Pi^u\sum\nolimits_{y\in\Psi}\sum\nolimits_G GP_u(\bar{y})\,y^{-a(y)}h_y, \quad (8)$$

where $\bar{y}$ denotes the distance between the user located at y from its serving UL BS and $\{\Pi^b,\Pi^u\}=\left\{\sum_{k=1}^{K}p_{kk}\pi_k^{\mathrm{F}}+\sum_{l>k}p_{kl},\delta^{\mathrm{F}}+(1-\delta^{\mathrm{F}})\delta^{\mathrm{U}}\right\}$ represent the fraction of interfering BSs and users, respectively. $I_{\mathrm{LI}}^{\mathrm{D}}$ and $I_{\mathrm{LI}}^{\mathrm{U}}$ denote the residual LI at the user and the BS, respectively, and are written as $I_{\mathrm{LI}}^{\mathrm{D}}=P_u(x_{\mathrm{U}})h_{\mathrm{LI}}$ and $I_{\mathrm{LI}}^{\mathrm{U}}=P_jh_{\mathrm{LI}}$.

C. Coverage probability

In this section, we investigate the coverage probability for both the DL and UL transmissions of the considered hybrid-duplex system. The coverage probability for $\mathcal{S}\in\{\mathrm{D},\mathrm{U}\}$ transmission $\mathcal{P}^{\mathcal{S}}(\tau^{\mathcal{S}})$, is the probability that the SINR is greater than a predefined threshold $\tau^{\mathcal{S}}$, and is given by

$$\mathcal{P}^{\mathcal{S}}(\tau^{\mathcal{S}})=\delta^{\mathrm{F}}\sum\nolimits_{i=1}^{K}\left(\left(p_{ii}\pi_i^{\mathrm{F}}+\sum\nolimits_{j>i}p_{ij}\right)\mathcal{P}_{ij}^{\mathcal{S}}(\tau^{\mathcal{S}})\right) + (1-\delta^{\mathrm{F}})\delta^{\mathcal{S}}\sum\nolimits_{i=1}^{K}p_i^{\mathcal{S}}\mathcal{P}_i^{\mathcal{S}}(\tau^{\mathcal{S}}), \quad (9)$$

where $\mathcal{P}_{ij}^{\mathcal{S}}(\tau^{\mathcal{S}})$ denotes the coverage probability for $\mathcal{S}\in\{\mathrm{D},\mathrm{U}\}$ of an FD user that is served by the BSs $r_i\in\Phi_i$ and $r_j\in\Phi_j$ for the DL and UL transmissions, respectively; $\mathcal{P}_i^{\mathcal{S}}$ represents the coverage probability of an HD user that is served by the BS $r_i\in\Phi_i$ for the $\mathcal{S}$ transmission. Based on the above, in the following subsections, we provide the coverage probability for the DL and UL directions.

1) Downlink: We denote by $\mathcal{P}_{ij}^{\mathrm{D}}(\tau^{\mathrm{D}})$ the DL coverage probability of a user that is served by the BSs $r_i\in\Phi_i$ and $r_j\in\Phi_j$ for the DL and the UL transmissions, respectively, and is given by $\mathcal{P}_{ij}^{\mathrm{D}}(\tau^{\mathrm{D}})=\mathbb{P}\left[\mathrm{SINR}_{ij}^{\mathrm{D}}>\tau^{\mathrm{D}}\right]$, where τ^{D} is the predefined threshold for the DL direction. The following theorem provides the achieved DL network performance.

Theorem 1. *The DL coverage probability $\mathcal{P}_{ij}^{\mathrm{D}}(\tau^{\mathrm{D}})$ in an FD cell, is given by*

$$\mathcal{P}_{ij}^{\mathrm{D}}(\tau^{\mathrm{D}})=\int_0^R\int_{\eta_{ij}(u,v)}^u\Lambda(s_{\mathrm{L}})f(u,v)\,dv\,du + \int_R^\infty\int_{\eta_{ij}(u,v)}^u\Lambda(s_{\mathrm{N}})f(u,v)\;dv\,du, \quad (10)$$

where $s=\{s_{\mathrm{L}},s_{\mathrm{N}}\}=\{\frac{\tau^{\mathrm{D}}u^{a_{\mathrm{L}}}}{M^2P_i},\frac{\tau^{\mathrm{D}}u^{a_{\mathrm{N}}}}{M^2P_i}\}$, $\Lambda(s)=\mathcal{L}_{I^{\mathrm{D}}}(sI^{\mathrm{D}})\,\mathcal{L}_{I_{\mathrm{LI}}^{\mathrm{D}}}(sI_{\mathrm{LI}}^{\mathrm{D}})\,e^{-s\sigma_n^2}$, *$f(u,v)$ is given by Lemma 3, $\eta_{ij}(u,v)=\left(\frac{P_j}{P_i}u^{a(u)}\right)^{a(v)}$ and the Laplace transforms of the received interference and the residual LI, are given by*

$$\mathcal{L}_{I^{\mathrm{D}}}(s)=e^{-2\pi\sum_G p_G\left(\sum_{k=1}^{K}\lambda_k\Pi^b\mathcal{Y}(u,sGP_k)+\lambda_u\Pi^u\sum_{\mathcal{S}}\mathcal{H}(\mathrm{D},0)\right)}, \quad (11)$$

$$\mathcal{Y}(\kappa,\beta)=\begin{cases}\frac{\beta(R\kappa)^{-a_{\mathrm{L}}}}{a_{\mathrm{L}}-2}\left(R^{a_{\mathrm{L}}}\kappa^2{}_2F_1\left[1,\frac{a_{\mathrm{L}}-2}{a_{\mathrm{L}}},2-\frac{2}{a_{\mathrm{L}}},-\kappa^{-a_{\mathrm{L}}}\beta\right]-R^2\kappa^{a_{\mathrm{L}}}{}_2F_1\left[1,\frac{a_{\mathrm{L}}-2}{a_{\mathrm{L}}},2-\frac{2}{a_{\mathrm{L}}},-R^{-a_{\mathrm{L}}}\beta\right]\right), & \kappa\le R,\\ \frac{\kappa^{2-a_{\mathrm{N}}}\beta}{a_{\mathrm{N}}-2}{}_2F_1\left[1,\frac{a_{\mathrm{N}}-2}{a_{\mathrm{N}}},2-\frac{2}{a_{\mathrm{N}}},-\kappa^{-a_{\mathrm{N}}}\beta\right], & \kappa>R.\end{cases} \tag{13}$$

$$\mathcal{H}(\mathcal{S},\kappa)=\int_{u\in\Phi^{\mathcal{S}}}\left(1-2\pi\lambda_u\left(\int_{\kappa}^{R}\frac{\bar{y}e^{-\pi\lambda_u\bar{y}^2}}{1+sGP_u(\bar{y},a_{\mathrm{L}})y^{-a_{\mathcal{S}}}}\,d\bar{y}+\int_{R}^{\infty}\frac{\bar{y}e^{-\pi\lambda_u\bar{y}^2}}{1+sGP_u(\bar{y},a_{\mathrm{N}})y^{-a_{\mathcal{S}}}}\,d\bar{y}\right)\right)u\,du. \tag{14}$$

and $\mathcal{L}_{I_{\mathrm{LI}}^{\mathrm{D}}}(s)=\left(1+\frac{sP_u(r_j)\sigma_{\mathrm{LI}}^2}{\mu}\right)^{-\mu}$*, where the expressions* $\mathcal{Y}(\kappa,\beta)$ *and* $\mathcal{H}(\mathcal{S},\kappa)$ *are given by* (13) *and* (14)*, respectively.*

Proof. See Appendix A. □

2) Uplink: We denote the UL coverage probability as $\mathcal{P}_{ij}^{\mathrm{U}}(\tau^{\mathrm{U}})$, and is given by $\mathcal{P}_{ij}^{\mathrm{U}}(\tau^{\mathrm{U}})=\mathbb{P}\left[\mathrm{SINR}_{ij}^{\mathrm{U}}>\tau^{\mathrm{U}}\right]$, where τ^{U} is the predefined threshold for UL. The following theorem provides the UL network performance.

Theorem 2. *The UL coverage probability* $\mathcal{P}_{ij}^{\mathrm{U}}(\tau^{\mathrm{U}})$ *in an FD cell, is given by* (10)*, where* $\Lambda(s)=\mathcal{L}_{I^{\mathrm{U}}}(sI^{\mathrm{U}})\,\mathcal{L}_{I_{\mathrm{LI}}^{\mathrm{U}}}(sI_{\mathrm{LI}}^{\mathrm{U}})\,e^{-s\sigma_n^2}$,

$$\mathcal{L}_{I^{\mathrm{U}}}(s)=e^{-2\pi\sum\limits_{G}p_G\left(\sum\limits_{k=1}^{K}\lambda_k\Pi^b\mathcal{Y}(0,sGP_k)+\lambda_u\Pi^u\sum\limits_{\mathcal{S}}\mathcal{H}(\mathrm{U},v)\right)},$$

and $\mathcal{L}_{I_{\mathrm{LI}}^{\mathrm{U}}}(s)=\left(1+\frac{sP_j\sigma_{\mathrm{LI}}^2}{\mu}\right)^{-\mu}$*, where* $\mathcal{Y}(\kappa,\beta)$ *and* $\mathcal{H}(\mathcal{S},\kappa)$ *are given by* (13) *and* (14)*, respectively.*

Proof. The proof follows similarly steps as the proof of Theorem 1. The proof is omitted due to space limitations. □

D. Sum-rate Performance

An equally important performance metric is the sum-rate performance (bits/sec/Hz). Using the coverage probability, we can now derive the average spectral efficiencies achieved by the FD and the HD users. By using Shannon's formula, the rate $\mathcal{R}^{\mathrm{F}}$ of an FD link for a user served by a BS from the i-th tier for DL and a BS from the j-th tier for UL, is defined as

$$\mathcal{R}^{\mathrm{F}}(\tau^{\mathrm{D}},\tau^{\mathrm{U}})=\sum_{i=1}^{K}\sum_{j\ge i}^{K}p_{ij}\sum_{\mathcal{S}}\mathcal{P}_{ij}^{\mathcal{S}}(\tau^{\mathcal{S}})\ln(1+\tau^{\mathcal{S}}). \tag{18}$$

On the other hand, the rate $\mathcal{R}^{\mathcal{S}}$ of an HD link for a user served by a BS from the i-th tier for $\mathcal{S}$ transmission, is defined as

$$\mathcal{R}^{\mathcal{S}}(\tau^{\mathcal{S}})=\sum_{i=1}^{K}p_i^{\mathcal{S}}\mathcal{P}_i^{\mathcal{S}}(\tau^{\mathcal{S}})\ln(1+\tau^{\mathcal{S}}). \tag{19}$$

In the following theorem, the sum-rate expression of the considered cellular networks is derived.

Theorem 3. *The sum-rate performance of the considered cellular networks, is given by*

$$\mathcal{R}(\tau^{\mathrm{D}},\tau^{\mathrm{U}})=\mathcal{R}^{\mathrm{F}}(\tau^{\mathrm{D}},\tau^{\mathrm{U}})+\mathcal{R}^{\mathrm{D}}(\tau^{\mathrm{D}})+\mathcal{R}^{\mathrm{U}}(\tau^{\mathrm{U}}). \tag{20}$$

Proof. By substituting (9) into the expressions (18) and (19) and by adding them up, the expression (20) follows. □

IV. Numerical Results

In this section, we provide numerical results to verify our model and illustrate the impact of implementing an FD-enabled mmWave cellular network. We focus on the special case of a heterogeneous network with $K=2$ tiers, where the density of the first and the second tier are $\lambda_1=8$ BSs/km^2 and $\lambda_2=20$ BSs/km^2, respectively; the transmit powers of the network tiers are $P_1=15$ dBm and $P_2=5$ dBm, respectively, and the fraction of BSs that operate in FD mode is $\pi_1^{\mathrm{F}}=\pi_2^{\mathrm{F}}=0.8$. The noise power is set to $\sigma_n^2=-90$ dBm. The path loss exponent of a LOS and a NLOS link is set to $a_L=3$ and $a_N=4$, respectively, and the maximum length of a LOS link is $R=100$ m [10]. The power control factor is $\epsilon=0.9$ and all BSs have the same receiver sensitivity $\rho=-40$ dBm. The parameters for the residual LI of FD nodes are $\sigma_{\mathrm{LI}}^2=-60$ dB and $\mu=4$, and for the sectorized antenna model are set to $M=10$ dB, $m=-10$ dB and $\theta=\frac{\pi}{6}$. For the evaluation of the performance metrics, we assume $\tau=\tau^{\mathrm{D}}=\tau^{\mathrm{U}}$, $\delta^{\mathrm{D}}=\delta^{\mathrm{U}}=0.5$ and $\delta^{\mathrm{F}}=0.5$.

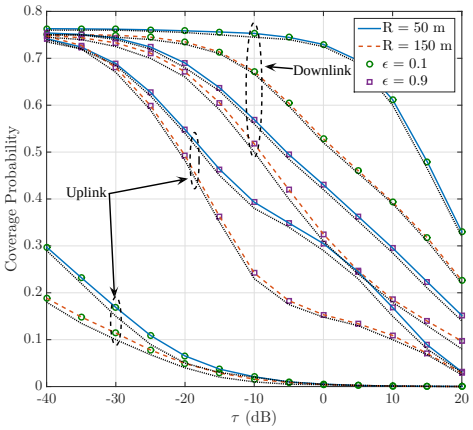

Fig. 1: Coverage versus τ for different ϵ and R; $\delta^{\mathrm{F}}=0.5$

Fig. 1 illustrates the effects of blockages and power control on the FD-enabled mmWave network performance. The first main observation is the positive effect of the blockages on the coverage probability for both the DL and UL transmissions. This observation was expected, since by reducing the amount of LOS interference, i.e. the density of blockages increases, the received interference becomes weaker and the received SINR is increased. Moreover, we can easily observe that as the power control factor increases, the DL coverage probability decreases and the UL coverage probability increases. This is explained by the fact that, by increasing the ability of the users in compensating the large-scale path loss, the users transmit with higher power levels. Thus, the received interference and the residual LI at the users are increased, resulting in a decreased SINR for the DL transmission. On the other hand, the received signal at the BSs is increased, resulting

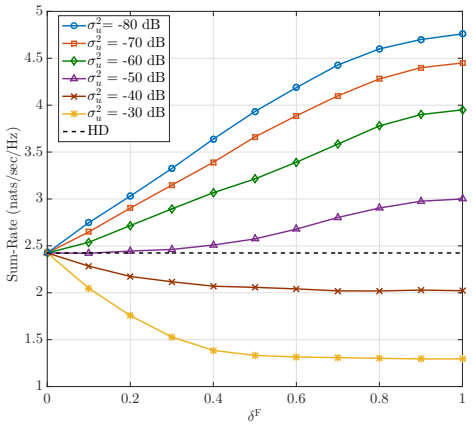

Fig. 2: Sum-rate versus δ^{F} for different residual LI; $\tau = 0$ dB.

in an increased SINR for the UL transmission. Finally, the figure shows that the analytical expressions for the DL and the UL coverage probabilities, perfectly match the simulation results, presented as dotted lines, and validate our theoretical derivations.

Fig. 2 shows the effect of the residual LI and the fraction of FD users on the network's sum-rate performance. We can easily observe that by increasing the ability of the users to cancel the LI, the sum-rate of the considered network is increased. This was expected since by decreasing the residual LI at the users, the received SINR and the sum-rate are increased. As expected, the sum-rate is independent from the ability of users to cancel the LI for the case where all the users operate in HD mode. Finally, it is clear from the figure that if the users have high LI cancellation capabilities, the highest sum-rate performance can be achieved when all the users are operating in FD mode. For the case where the users have low LI cancellation capabilities, all the users must operate in HD mode in order to achieve the highest sum-rate performance.

V. Conclusion

In this paper, we studied the performance of FD radio in heterogeneous mmWave cellular networks. We proposed a stochastic geometry-based model that allowed us to theoretically assess the coverage and sum-rate performance, for both the DL and the UL directions. Both the coverage and the sum-rate performance were derived in analytical expressions and the impact of blockage density, power control, residual LI and fraction of FD users, have been discussed. We have shown that mmWave cellular networks provide to FD radio an ideal environment in which it doubles the network's spectral efficiency, while combating the severe interference via mmWave characteristics. A future extension of this work is to investigate the energy efficiency of the considered FD-capable heterogeneous mmWave cellular networks.

Appendix A

The DL coverage probability of a user that is served by the BSs $r_i \in \Phi_i$ and $r_j \in \Phi_j$ for the DL and the UL transmissions, respectively, is given by

$$\mathcal{P}_{ij}^{\mathrm{D}}\left(\tau^{\mathrm{D}}\right) \overset{(a)}{=} \mathbb{E}\left[\exp\left(-s\left(I^{\mathrm{D}} + I_{\mathrm{LI}}^{\mathrm{D}} + \sigma_n^2\right)\right)\right] \overset{(b)}{=} \mathbb{E}_{r_i, r_j}\left[\mathcal{L}_{I^{\mathrm{D}}}\left(sI^{\mathrm{D}}\right)\mathcal{L}_{I_{\mathrm{LI}}^{\mathrm{D}}}\left(sI_{\mathrm{LI}}^{\mathrm{D}}\right)e^{-s\sigma_n^2}\right],$$

where $s = \frac{\tau^{\mathrm{D}} r_i^{a(r_i)}}{M^2 P_i}$ and (a) follows from the fact that $|h_u|^2$ is an exponential random variable with mean $M^2 P_i r_i^{-a(r_i)}$. In (b), we make use of the Laplace transform of I^{D} and $I_{\mathrm{LI}}^{\mathrm{D}}$, where $\mathcal{L}_{I^{\mathrm{D}}} = \mathbb{E}\left[\exp(-sI^{\mathrm{D}})\right]$ and $\mathcal{L}_{I_{\mathrm{LI}}^{\mathrm{D}}} = \mathbb{E}\left[\exp(-sI_{\mathrm{LI}}^{\mathrm{D}})\right]$, respectively. Using (8), the Laplace transform of the received interference I^{D}, $\mathcal{L}_{I^{\mathrm{D}}}(s)$, can be re-written as

$$\mathcal{L}_{I^{\mathrm{D}}}(s) = \prod_{k=1}^{K} e^{-2\pi\lambda_k \Pi^b \sum_G p_G \int_{r_i}^{\infty}\left(1-\frac{1}{1+sGP_k u^{-a(u)}}\right)u\,du} \times e^{-2\pi\lambda_u \Pi^u \sum_G p_G \int_0^{\infty}\left(1-\mathbb{E}_{\bar{y}}\left[\frac{1}{1+sGP_u(\bar{y})y^{-a(y)}}\right]\right)y\,dy},$$

which follows from the probability generating functional of a PPP [10]. It is important to note here that, the area in which the interfering BSs are located, depends on the location of the serving BS. Specifically, if the location of the serving BS is $r_i \leq R$, then the interfering BSs are located in $\{r_i, R\} \cup \{R, \infty\}$, otherwise, they are in $\{r_i, \infty\}$. On the other hand, all users, irrespective of the link status $\mathcal{S} \in \{\mathrm{L}, \mathrm{N}\}$, are causing interference to the typical user. Thus, the Laplace transform of the received interference is given by (11) and the expressions $\mathcal{Y}(\kappa, \beta)$ and $\mathcal{H}(\mathcal{S}, \kappa)$ are formed as in (13) and (14), respectively. The Laplace transform of the LI can be written as $\mathcal{L}_{I_{\mathrm{LI}}^{\mathrm{D}}}(s) = \mathbb{E}\left[e^{-sP_u(r_j)|h_u|^2}\right]$, and by using the moment generating function of the gamma random variable $|h_u|^2$, the expressions in Theorem 1 are derived.

References

[1] G. A. Akpakwu, B. J. Silva, G. P. Hancke, and A. M. Abu-Mahfouz, "A survey on 5G networks for the internet of things: Communication technologies and challenges," in *IEEE Access,* vol. 6, pp. 3619–3647, 2018.

[2] N. H. Mahmood, M. G. Sarret, G. Berardinelli, and P. Mogensen, "Full duplex communications in 5G small cells," *13th Int. Wireless Commun. Mobile Computing Conf.,* Valencia, 2017, pp. 1665–1670.

[3] I. Atzeni and M. Kountouris, "Full-duplex MIMO small-cell networks with interference cancellation," *IEEE Trans. Wireless Commun.,* vol. 16, pp. 8362–8376, Dec. 2017.

[4] J. Lee and T. Q. S. Quek, "Hybrid full-/half-duplex system analysis in heterogeneous wireless networks," *IEEE Trans. Wireless Commun.,* vol. 14, pp. 2883–2895, May 2015.

[5] J. Lee and T. Q. S. Quek, "Hybrid full-/half-duplex system analysis in heterogeneous wireless networks," *IEEE Trans. Wireless Commun.,* vol. 14, pp. 2883–2895, May 2015.

[6] Z. Xiao, P. Xia, and X. G. Xia, "Full-duplex millimeter-wave communication," *IEEE Wireless Commun.,* vol. 24, pp. 136–143, Dec. 2017.

[7] Z. Wei, X. Zhu, S. Sun, Y. Huang, A. Al-Tahmeesschi, and Y. Jiang, "Energy-efficiency of millimeter-wave full-duplex relaying systems: challenges and solutions," *IEEE Access,* vol. 4, pp. 4848–4860, Jun. 2016.

[8] A. AlAmmouri, H. ElSawy, O. Amin, and M. S. Alouini, "In-band α-duplex scheme for cellular networks: A stochastic geometry approach," *IEEE Trans. Wireless Commun.,* vol. 15, pp. 6797-6812, July 2016.

[9] C. Skouroumounis, C. Psomas, and I. Krikidis, "Heterogeneous FD-mmWave cellular networks with cell center/edge users," *IEEE Trans. Commun.*, to be published.

[10] J. G. Andrews, T. Bai, M. Kulkarni, A. Alkhateeb, A. Gupta, and R. W. Heath, "Modeling and analyzing millimeter wave cellular systems," *IEEE Trans. Commun.,* vol. 65, pp. 403-430, Jan. 2017.